

# Hydroxyapatite scaffolds for bone tissue engineering made by 3D printing

BARBARA LEUKERS<sup>1</sup>, HÜLYA GÜLKAN<sup>2</sup>, STEPHAN H. IRSEN<sup>1</sup>, STEFAN MILZ<sup>3</sup>, CARSTEN TILLE<sup>1</sup>, MATTHIAS SCHIEKER<sup>2</sup>, HERMANN SEITZ<sup>1</sup>

<sup>1</sup>Research Center Caesar, Ludwig-Erhard-Allee 2, 53175 Bonn

<sup>2</sup>Experimental Surgery and Regenerative Medicine, Department of Surgery—Downtown, University of Munich, Nussbaumstrasse 20, 80336 München

<sup>3</sup>AO Research Institute, Clavadelerstrasse, 7270 Davos, Switzerland

Nowadays, there is a significant need for synthetic bone replacement materials used in bone tissue engineering (BTE). Rapid prototyping and especially 3D printing is a suitable technique to create custom implants based on medical data sets. 3D printing allows to fabricate scaffolds based on Hydroxyapatite with complex internal structures and high resolution. To determine the *in vitro* behaviour of cells cultivated on the scaffolds, we designed a special test-part. MC3T3-E1 cells were seeded on the scaffolds and cultivated under static and dynamic setups. Histological evaluation was carried out to characterise the cell ingrowth. In summary, the dynamic cultivation method lead to a stronger population compared to the static cultivation method. The cells proliferated deep into the structure forming close contact to Hydroxyapatite granules.

© 2005 Springer Science + Business Media, Inc.

## 1. Introduction

Synthetic bone replacement materials based on Calciumphosphates are widely used in clinically routine [1]. A synthetic scaffold for bone tissue engineering requires an inner structure with interconnecting pores. Pore sizes with diameters above 300  $\mu\text{m}$  are recommended to promote good vascularisation and attachment of bone cells to guide their growth into all three dimensions [2]. The use of rapid prototyping (RP) allows the production of scaffolds with defined and reproducible internal structures directly from computer data [3]. Furthermore, the outer shape of the scaffold can be designed by taking anatomical information of the patient's target defect (e.g. CT scan, MRI images) to obtain a custom-tailored implant. We use the RP process 3D printing, developed at the Massachusetts Institute of Technology (MIT) [4]. The main advantage of this technique is, that an implant can be manufactured straight from a 3D data set in one step without using an additional mold. We use Hydroxyapatite (HA) granulates to fabricate porous ceramic structures with designed internal architecture. HA is a promising bone replacement material because of its stoichiometric similarity to the inorganic part of natural bone. The fabrication process itself [5] as well as studies about various HA granulates for 3D printing were objectives of earlier studies and will be published elsewhere [6].

The matrices generated by 3D printing can be used for bone tissue engineering using patient's cells seeded onto the scaffolds. The scaffolds serve as three-dimensional templates for initial cell attachment

and subsequent tissue formation. For this reason it is important to ensure the cell ingrowth into the structure.

This study focuses mainly on scaffold design for histological evaluation of the seeded scaffolds. To optimize the seeding efficiency and to observe the cell proliferation into the inner structure, we developed a special design of the scaffold. The objective of the design was maximization of the surface, facilitation of the seeding process to enhance cell adhesion and good supply of the interior of the scaffold with medium.

The cultivation of cells seeded onto the scaffolds was carried out under static and dynamic conditions. Histological evaluation was carried out at day 1 and day 7. Cell adhesion on the designed structure was analysed. Additionally, cell ingrowth into the bulk material and cell morphology were examined.

## 2. Material and methods

### 2.1. Manufacturing process

3D printing requires a 3D dataset for the fabrication process. These data can originate from medical imaging sources or CAD programs. Since 3D printing generates physical models layerwise, the 3D dataset has to be converted into 2D data by a special slice algorithm. Afterwards, the 3D printer uses these 2D data to create a physical model, which is a 1:1 copy of the computer model. The 3D printing test setup that we used is shown in Fig. 1. The image shows the print-head of

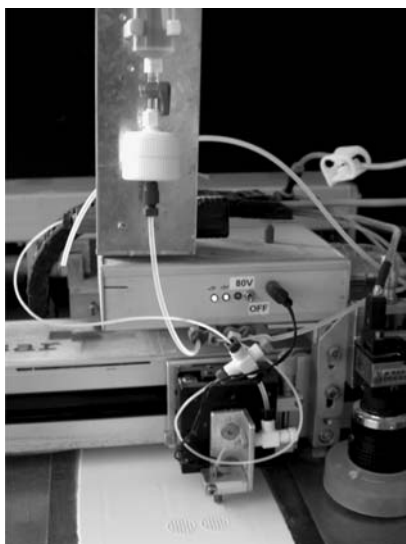


Figure 1 Experimental 3D printing test platform.

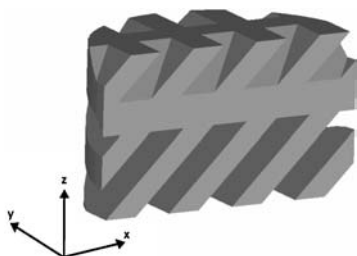


Figure 2 Test structure designed for histological evaluation. The image shows the vertical cross-section of the CAD model.

the device at work printing a 2D layer onto the powder bed. The building platform (showed in the lower part of the image) has a dimension of  $100 \times 100 \text{ mm}^2$ . The 3D printing process works as following: A defined layer of HA granulate is deposited on the building platform. A microdispensing valve ejects binder onto the powder surface and bonds the granules in the selected regions. After each printed layer the platform is lowered according to the layer thickness and new ceramic powder is deposited on the former layer. After finishing the whole process, slight airflow is used to remove unbound powder that remained in the internal structure of the part. Our test setup is very flexible in the means of investigat-

ing new process techniques and material combinations. In this study we used a spray-dried HA-granulate (V5) containing polymeric additives to improve bonding and flowability. A water soluble polymer blend (Schelofix) was used as binder. The materials were obtained from the Friedrich-Baur-Institute (FBI, Bayreuth, Germany). To achieve sufficient strength of the test bodies and to remove the organic binder compound, scaffolds were sintered for 2 h at  $1300^\circ\text{C}$  in a high temperature furnace.

## 2.2. Cell biology tests

For histological evaluation we designed a special test-part using standard CAD software which is shown in vertical cross-section view in Fig. 2. The internal structure of this scaffold has been made up of walls that all stand in  $45^\circ$  to the  $x$ -axis. The distance between two parallel walls is 1.2 mm and the calculated surface of the scaffold is  $1040 \text{ mm}^2$ .

$5 \times 10^4$  MC3T3-E1 murine fibroblasts (DSZM, Braunschweig, Germany) contained in  $600 \mu\text{l}$  suspension were seeded onto the scaffolds to enable covering of the scaffolds. During the first 2 h, the cell suspension was resuspended every 20 min and the scaffolds subsequently turned. This procedure was repeated once an hour for the next 2 to 3 h. At last, the test structures were incubated for 1 h and afterwards transferred into a new cavity of a 48 well plate for cultivation. Seeding efficiency was calculated by counting the number of cells remaining in the 48 well cavity where the seeding was carried out. For static subculture the scaffolds were cultivated in a 48 well plate whereas dynamic cultivation was performed in perfusion containers (MINUCELLS and MINUTISSUE GmbH, Bad Abbach, Germany). A flow rate of  $18 \mu\text{l}/\text{min}$  was adjusted. On day 1 and day 7 after cell seeding, scaffolds were embedded into methyl methacrylate (MMA) for histological evaluation. The MMA blocks were hardened for approx. 7 days and sectioned orthogonal to the flat surface of the scaffolds at  $100 \pm 10 \mu\text{m}$  using a saw microtome (Leica SP1600, Bensheim, Germany).

For visualization of cells and nuclei, sections were stained with paragon. Slices of the inner and outer part of the scaffolds were examined under a light microscope.

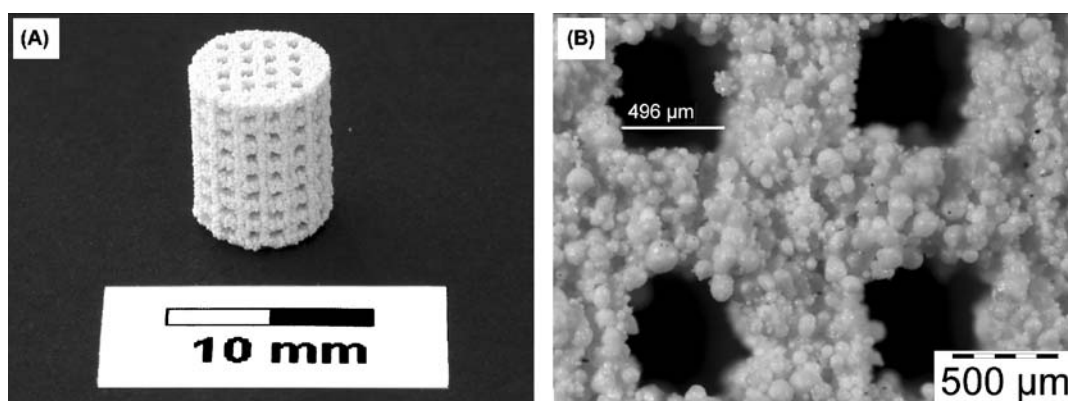


Figure 3 3D printed testpart with interconnecting channels. (a) Whole structure. (b) Detail view of the interconnecting channel structure with diameter of about  $500 \mu\text{m}$ . The remaining granule structure is visible.

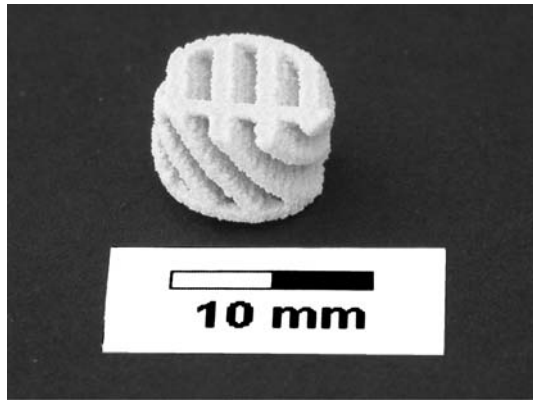


Figure 4 3D printed scaffold after sintering.

### 3. Results and discussion

The 3D printing test setup we used in this study allows to fabricate high resolution channel structures as required for BTE. Interconnecting channels with mean

diameters of about  $500\ \mu\text{m}$  could be realized. Fig. 3(a) depicts a 3D printed scaffold with an internal channel network. Fig. 3(b) shows that the granule structure remains after sintering. This leads to parts with high microporosity.

The 3D printed test structure we designed for histological evaluation is shown in Fig. 4. The shrinkage of the test structure after sintering was about 18–20% in all directions. The scaffold was stable and no distortion was detectable.

We have chosen a scaffold design with inclined layers of  $45^\circ$ . The aim of this specific design was to facilitate the seeding process and enhance cell attachment because the cells are hindered from sliding down of the structure. Additionally, the scaffold enables cell proliferation into the inside of the structure without clogging. Furthermore, good supply of the interior with nutrients should be ensured during cultivation. With this designed test structure and a modified cell seeding protocol, seeding efficiency was improved. By extending

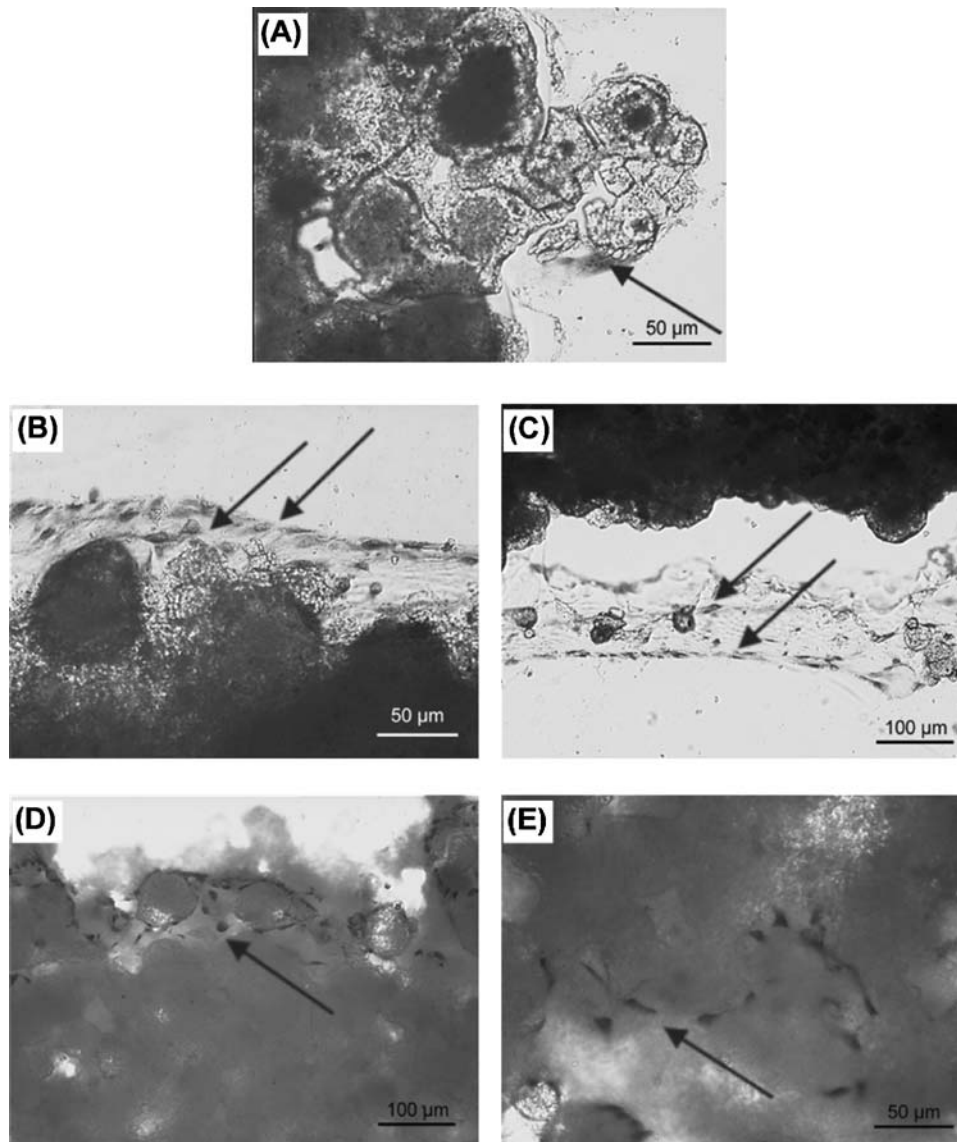


Figure 5 Paragon stained cross section of HA scaffolds seeded with MC3T3-E1 cells. Grey areas represent HA granules whereas Paragon stained cells (cytoplasm and cell nuclei) are visible as small spots showing single cells or cell layers, respectively. In detail figures (A) to (E) show: (A) statically cultured for 1 day: only one single cell visible (arrow); (B) outer slice and (C) inner slice of statically cultured cells after 7 days: cells grow layerwise; (D) outer slice and (E) inner slice of dynamically cultured cells for 7 days: deep cell ingrowth in between the HA-granules.

the seeding time to an overall of 5 to 6 h we obtained seeding efficiencies of approximately 82%.

To assess cell proliferation and cell growth behaviour of statically and dynamically cultured HA scaffolds, we performed a systematic histological analysis of slides taken from the inner and outer part of the scaffold at day 1 and day 7. On day 1 of culture, paragon staining revealed the presence of isolated cells spread over the scaffold surfaces. In all evaluated scaffolds, only single cells could be observed in statically and in dynamically cultured structures as shown in Fig. 5(a) for static cultivation. After one week in culture, the quantity of cells increased in both cultivation methods. Fig. 5(b) and 5(d) show the outer slice of the scaffold, whereas Fig. 5(c) and 5(e) show the inner slices. In both cultivation methods cells populated the outer and inner surface of HA scaffold by forming a continuous sheet that followed the scaffold contour. Nevertheless the two cultivation methods were clearly distinguishable with respect to cell growth behaviour on the HA granules. Static cells culture led to multiple cell layers located mostly on the surface of the HA granules as shown in Fig. 5(b) and (c). On dynamically cultured HA structures, cells tended to grow in between cavities of the granules (Fig. 5(d) and 5(e)). This type of growth was significantly different from that of statically cultured cells. The perfusion cell system seems to facilitate the supply with nutrients leading to better ingrowth of cells into the scaffolds' cavities. An alternative explanation might be that cells on HA scaffolds have grown deep into the cavities between HA granules to take shelter from the fluid shear forces caused by a flow rate of 18  $\mu\text{l}/\text{min}$  [7]. In contrast, the results of the paragon staining also showed that cells didn't seem to be damaged because of shear stress applied by the fluid flow. Both approaches definitely demonstrate that cells maintain their characteristic cell morphology. They attached well on 3D printed scaffolds and showed good proliferation into the HA matrices.

These findings are important for bone tissue engineering with mesenchymal stem cells, because the differentiation capabilities of cells seeded onto HA scaffolds should be retained for a certain period of culture in order to achieve a better outcome.

Moreover, the microporosity caused by the powder based 3D printing process, increases the scaffold surface accessible for fluid medium and thus for dissolution. This porosity is supposed to improve the remodeling process [8]. Osteoclasts have to attach tight to the

granule surface of the scaffold. By that, HA-crystals can be easily solubilized in the acid environment caused by the proton pump of the osteoclasts [9].

#### 4. Conclusions

In summary, cells proliferated well on our designed scaffolds in static and dynamic cultivation methods. Moreover, the perfusion system revealed that the cells grew deep in between the HA granules. HA scaffolds, made by 3D printing, are very suitable for bone replacement. Altogether, the findings of this presented study are important with respect to further application of 3D printed scaffolds for bone tissue engineering. Our future work will focus on the osteogenic differentiation capability of mesenchymal stem cells seeded on scaffolds with highly interconnecting channels.

#### Acknowledgments

This work has been supported by ForTePro (Bayerischer Forschungsverbund für Tissue Engineering und Rapid Prototyping) funded by the Bayerische Forschungsförderung. We gratefully thank the Friedrich-Baur-Research Institute for Biomaterials for supporting us with granulates and binder.

#### References

1. D. TADIC and M. EPPLE, *Biomaterials* **25** (2003) 987.
2. V. KARAGEORGIOU and D. KAPLAN, review, *ibid.* **26** (2005) 5474.
3. S. YANG, K. F. LEONG, Z. H. DU and C. H. CHUA, *Tissue Engineering* **8**(1) (2002) 1.
4. S.-J. J. LEE, E. SACHS and M. CIMA, *Rapid Prototyping Journal* **1**(4) (1995) 24.
5. H. SEITZ, W. RIEDER, S. H. IRSEN, B. LEUKERS, and C. TILLE, *J. Biomed. Mater. Res. Part B: Appl. Biomater.* in print.
6. S.H. IRSEN, U. DEISINGER, B. LEUKERS, W. RIEDER, S. SCHELER, F. STENZEL, G. ZIEGLER, C. TILLE and H. SEITZ, *J. Biomed. Mater. Res. Part B: Appl Biomater* submitted.
7. G. N. BANCROFT, M. D. V. I. SIKAVITSAS and A. G. MIKOS, *Tissue Engineering* **9** (2003) 549.
8. V. OLIVIER, N. FAUCHEUX and P. HARDOUIN, review, *Drug Discovery Today* **9**(18) (2004) 803.
9. S. C. MARKS and S. N. POPOFF, *The Amer. J. of Anatomy* **183** (1988) 1.

Received 30 June

and accepted 19 August 2005